Science and Technology Publishing (SCI & TECH)
ISSN: 2632-1017
Vol. 8 Issue 1, January - 2024

Development Of Thyristors-Based Direct-On-Line Starter For 3-Phase Electric Motor

Edet, Uduak Okon[1]
Department of Electrical and Electronic Engineering,
Akwa Ibom State University,
Ikot Akpaden, Akwa Ibom State Nigeria

Gabriel Umoh[2]
Department of Electrical and Electronic Engineering,
Akwa Ibom State University,
Ikot Akpaden, Akwa Ibom State Nigeria

Ubong S. Ukommi[3]
Department of Electrical and Electronic Engineering,
Akwa Ibom State University,
Ikot Akpaden, Akwa Ibom State Nigeria
uukommi@yahoo.com

Ekom E. Okpo[4]
Department of Electrical and Electronic Engineering,
Akwa Ibom State University,
Ikot Akpaden, Akwa Ibom State Nigeria

***Abstract*— In this work, development of thyristors-based direct-on-line starter for 3-phase electric motor is presented. Specifically, the Thyristor-based Direct On-Line (DOL) Starter is meant to control and thereby reduce or eliminate the motor startup problems identified in existing conventional Direct On-Line Starter and also provide an optimal solution to induction motor starters. The two major challenges identified in existing conventional Direct On-Line Starter are voltage sag and large inrush currents. The methodology included the system model development, the development of the model for the control strategy in the Thyristor-based Direct On-Line (DOL) Starter. The system is also modeled and simulated in MATLAB. The Thyristor-based solution is designed to be applicable to systems with various voltages levels ranging from $380V$ up to $10kV$.The simulation results showed that when the three phase electric motor is operated using the conventional method, there is a large inrush starting current of up to $3700A$ at the initial stage which goes gradually to steady state in about $10\,seconds$. However, when the proposed solution is applied, the current waveform does not just have a quick settling time (at about 0.3 seconds), but the settling amplitude is about $150A$ which is about 70% improvement. Also, with the existing conventional starter method the line current oscillates initially around $\pm 800A$, then settles at steady state around $\pm 180A$ in $0.2\,seconds$. However, with the proposed Thyristor-based method, the current tends to begin from zero and then rise to attend a steady state of about $\pm 220A$ in 0.08 seconds. The current starts from zero in the conventional case following the running speed of the rotor. On the other hand, the proposed method does not engage motor system until the current rises to a sufficient magnitude. This makes it safe for loads connected to the system. In addition, the results for the system line currents, electromagnetic torque and rotor speed at normal operation (or steady state) show that the proposed system behaviours do not differ from the existing or convention system at steady state. Notably, the Thyristor-based method presented in this work is only relevant when the three phase electric motor is about to start. This is the time it draws enormous current, and the aim of this study is to minimize the huge current (using the soft start technique). As such, once the three phase electric motor is started and runs on normal operating speed, everything becomes normal as is obtainable in the phase electric motor with the conventional starter method.**

***Keywords*— Direct-On-Line Starter, Thyristors, Electronic Starter, 3-Phase Electric Motor, Rotor Resistance Starter, Stator Resistance Starter**

1.0 INTRODUCTION

In many industries today, three phase electric motor are prime movers of major processes [1]. Importantly, three phase electric motor mainly works based on the principles of rotating magnetic field [2,3]. More often, the motor windings get damaged due to large amount of inrush current during startup of the motor [4,5]. Consequently, there is a significant amount of voltage drop in the line, thus subjecting other components which share the same line to voltage spikes. One of the effective ways to eliminate or reduce such unwanted effect is to limit the current drawn by the three phase electric motor at the starting period. The mechanism used to minimize the initial inrush current at startup is known as the starter, which typically reduces the supply voltage to the three-phase motor. It is expected that the reduced voltage is sustained until motor reaches the rated speed before the rated voltage is applied [6,7]. Various studies have revealed that Star-Delta Starters, Autotransformer Starter, Direct Online Starter (DOL), Electronic Starter, Rotor Resistance Starter, and Stator Resistance Starter, are commonly used starters. However, this work considers the SCR DOL based controller [8,9,10].

Specifically, this work proposes a DOL starter circuit based on SCR technology to address the issues identified from the existing methods [11,12]. Based on the reviewed literatures, the major work gaps discovered include over-voltage, over-current, voltage sags, jerking, mechanical wearing and electrical wearing. Consequently, emphasis is laid on these parameters as they form the key metrics of the design.

2. METHODOLOGY

The central focus of this research is on the design of electric circuitry for Thyristor-based Direct On-Line (DOL) Starter for three phase electric motor. It is the process of integrating electromechanical components such as Isolator Gear Switch Fuses (IGSF), Model Case Circuit Breaker (MCCB), Thermal Overload Relay (TOR) and electronic components such as Capacitor, Inductor, Rectifier and Thyristor known as Silicon Controlled Rectifier(SCR) to actualized the thyristo-based Direct On-Line Starter for three phase induction motor [13]. The proposed Thyristor-based Direct On-Line (DOL) Starter is meant to control and thereby reduce or eliminate the motor startup problems identified in existing conventional Direct On-Line Starter and also provide an optimal solution to induction motor starters. The methodology included the system model development, the development of the model for the control strategy in the Thyristor-based Direct On-Line (DOL) Starter. Eventually, the model simulation and performance evaluation are presented followed by results and discussions.

2.1 The System Model

Silicon Controlled Rectifier (SCR) is one of the major component of an electronic starter which is also considered as soft starter [14,15]. In this design, the SCR voltage controllers are used of which the block diagram is presented in Figure 1.

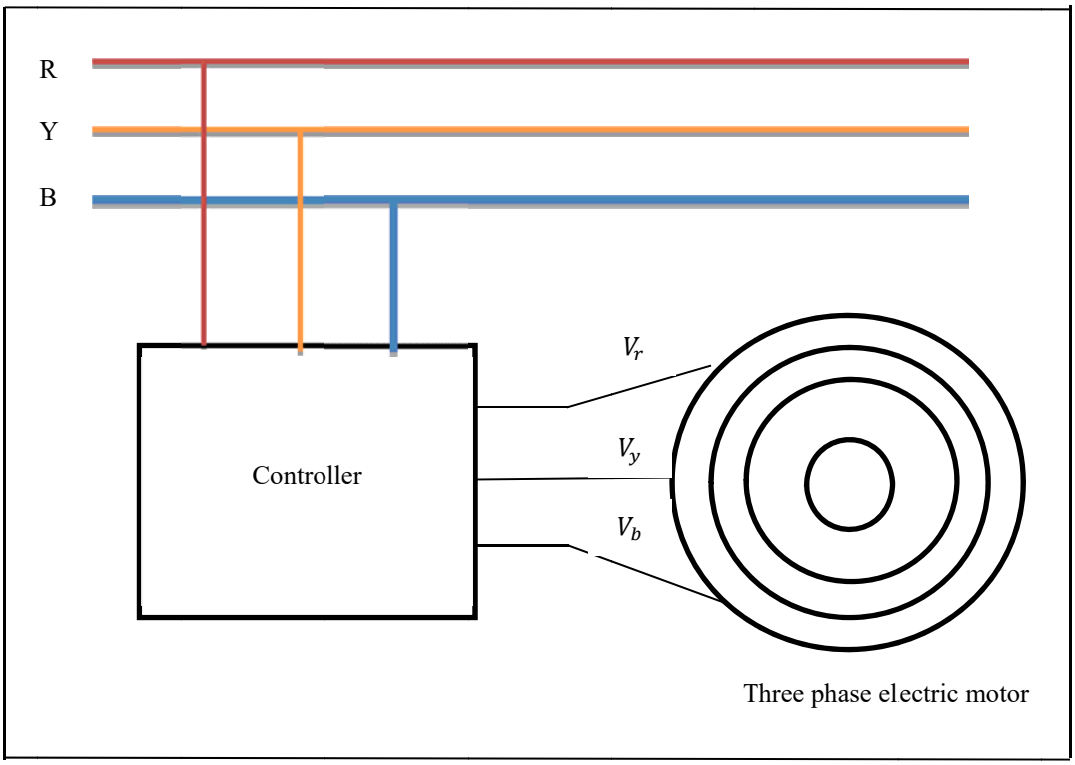

Figure 1: The Basic Block Diagram for Voltage Control Scheme

As shown in Figure 1, the three-phase supply is connected to the three-phase electric motor through the controller in which one of the primary components is SCR. In this design, two SCRs are connected in series in each line to control the voltage supplied to the stator, while the SCR firing angle is also controlled adequately. The SCRs are biased such that they conduct alternately; during the first half of the signal cycle, one SCR conducts while the other is shut down throughout the first half period. During the second half of signal period, the SCR that was previously turned on is turned off while the other is turned on. The voltage supplied to the motor is effectively controlled by controlling the firing angle of the SCRs.

The controller unit of Figure 1 consists of contactors and sensors. The essence of contactors in the design is to bypass the soft starter unit when the motor attains its rated speed. Secondly, contactors help to minimize the harmonics and power loss in the system. The sensors basically check the starting current, supply voltage and terminal voltage, which are the requirements for the firing operation of the SCR.The firing angle of the SCR can be calculated from Equation 1.

$$\alpha_{phase} = \alpha_T - \alpha_V - \alpha_I \quad (1)$$

Where α_T denotes the terminal voltage, α_V denotes the supply voltage, and α_I denotes the starting current. The relationship between the rms voltage and the firing angle of the SCR can be expressed as:

$$K_{\alpha_V} = \frac{V_{rms}}{\alpha_V} \quad (2)$$

$$K_{\alpha_I} = \frac{V_{rms}}{\alpha_V} \quad (3)$$

Where K_{α_V} and K_{α_I} are gain constant for voltage and current respectively.

Since SCR based switches are vulnerable to issues such as low utilization efficiency, this research considers integrating a series inverter along with the control unit. Hence, a series compensator (SC) method is proposed in this

study. The proposed configuration model is presented in Figure 2. The equivalent circuit of a typical induction motor and the proposed system are presented in Figure 3 and Figure 4 respectively.

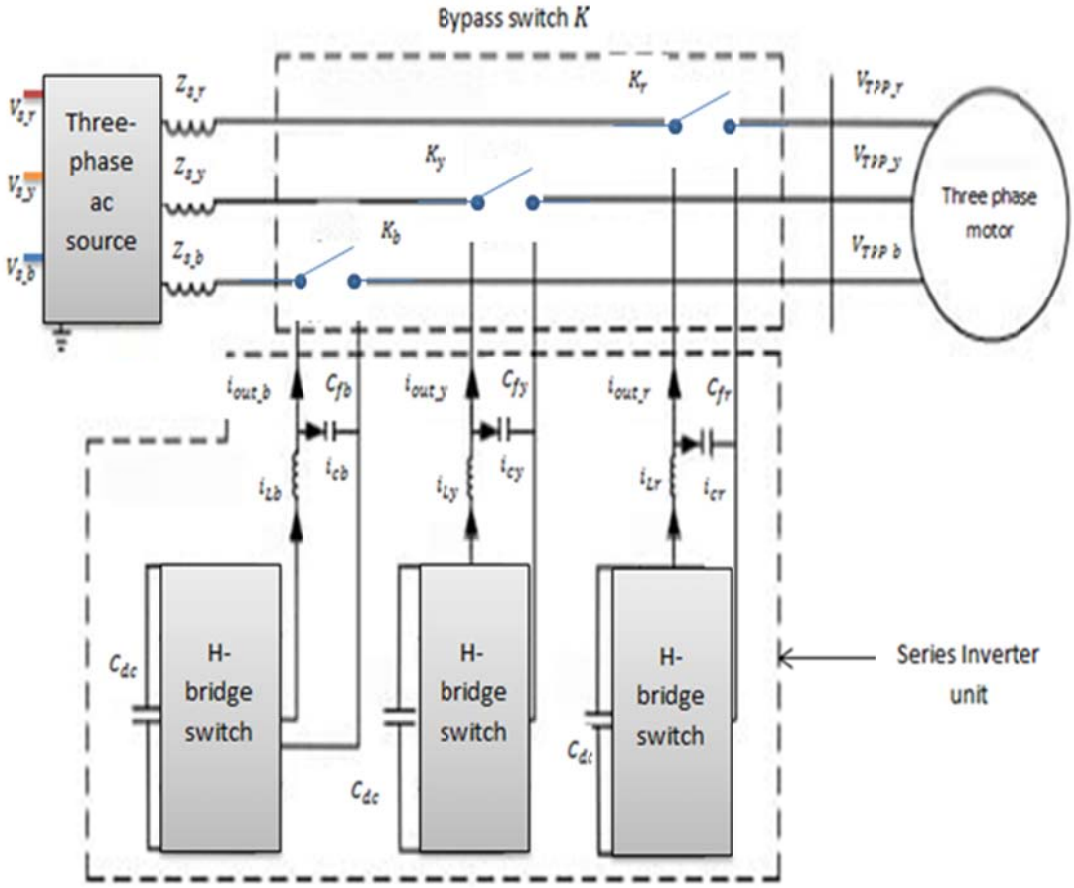

Figure 2: Circuit Configuration of the Proposed Series Compensator

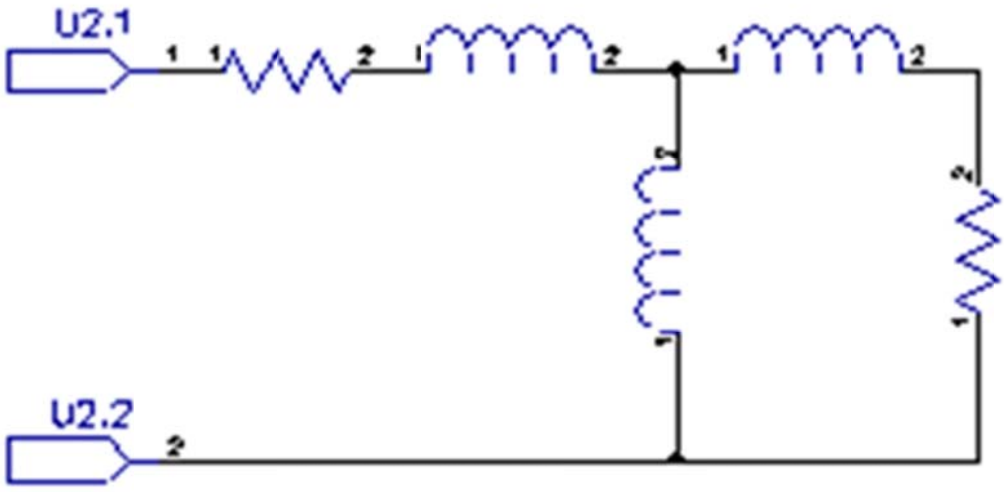

Figure 3: Equivalent circuit of a three-phase motor.

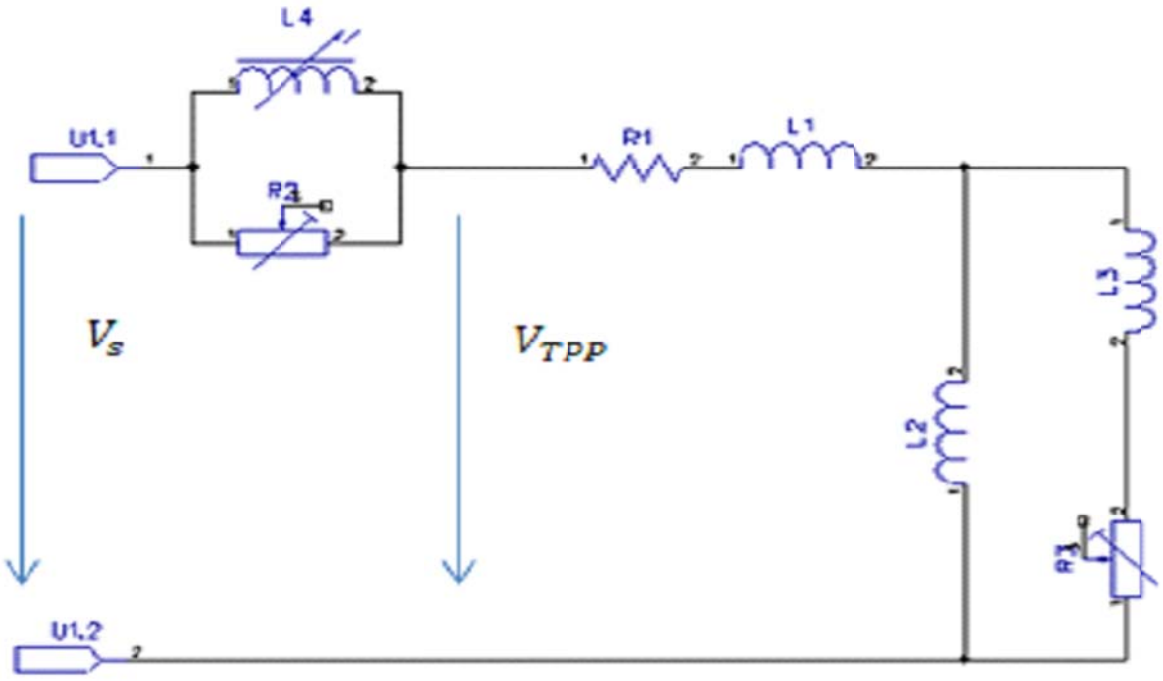

Figure 4: Equivalent circuit of a three-phase motor with the proposed series compensator system

These equivalent circuits are used to compute the electrical parameters of the induction motors based on various modes. From Figure 4, the equivalent impedance of the induction motor Z_{equiv} can be expressed as:

$$Z_{equiv} = (R_{stator} + X_{stator}i) + \frac{(X_m i)\left(\frac{R_{rotor}}{s_p} + X_{rotor}i\right)}{(X_m i) + \left(\frac{R_{rotor}}{s_p} + X_{rotor}i\right)} \quad (4)$$

Where, R_{stator} denotes the stator resistance, X_{stator} denotes stator leakage reactance, X_m denotes the magnetizing reactance, R_{rotor} denotes the rotor resistance, X_{rotor} denotes rotor leakage reactance, s_p denotes slip, and i is a complex number. The current on the stator side can be expressed as:

$$i_{stator} = \frac{V_{TPP}}{Z_{equiv}} \quad (5)$$

Where, V_{TPP} denotes terminal voltage per phase. By introducing Equation 4 into Equation 5, the stator current can be rewritten as:

$$i_{stator} = \frac{V_{TPP}}{(R_{stator} + X_{stator}i) + \frac{(X_m i)\left(\frac{R_{rotor}}{s_p} + X_{rotor}i\right)}{(X_m i) + \left(\frac{R_{rotor}}{s_p} + X_{rotor}i\right)}} \quad (6)$$

Electromagnetic torque is given as:

$$T_{em} = \frac{3I'^2_{rotor}R_{rotor}}{s_p} \cdot \frac{p}{4\pi f} \quad (7)$$

Where, p denotes the number of poles of the motor, I'_{rotor} denotes rotor current at the stator side, $3I'^2_{rotor}R_{rotor}$ denotes the electromagnetic power P_{em}, and f is the frequency. Since I'^2_{rotor} can be expressed according to ohm's law as:

$$I'^2_{rotor} = V^2_{TPP}\left|\frac{X_m i}{\alpha + \beta i}\right| \quad (8)$$

The electromagnetic torque can be rewritten as:

$$T_{em} = \frac{3pR_{rotor}}{4\pi f s_p} \cdot V^2_{TPP}\left|\frac{X_m i}{\alpha + \beta i}\right| \quad (9)$$

Where, α and β can be expressed as:

$$\begin{cases} \boldsymbol{\alpha} = \frac{\boldsymbol{R_{stator}} \cdot \boldsymbol{R_{rotor}}}{\boldsymbol{s_p}} - \boldsymbol{X_{stator}} \cdot \boldsymbol{X_{rotor}} - \boldsymbol{X_m}(\boldsymbol{X_{stator}} + \boldsymbol{X_{rotor}}), \\ \boldsymbol{\beta} = \boldsymbol{R_{stator}} \cdot \boldsymbol{X_{rotor}} + \frac{\boldsymbol{R_{rotor}} \cdot \boldsymbol{X_{stator}}}{\boldsymbol{s_p}} + \boldsymbol{X_m}\left(\boldsymbol{R_{stator}} + \frac{\boldsymbol{R_{rotor}}}{\boldsymbol{s_p}}\right) \end{cases} \quad (10)$$

Equation 9 can be rewritten as:

$$T_{em} = \frac{3pR_{rotor}}{4\pi f s_p} \cdot \left| \frac{X_m i}{\frac{R_{rotor}}{s_p} + (X_{rotor} + X_m)i} \right| \cdot I_s^2 \quad (11)$$

Equation 11 expresses the electromagnetic torque as a function of stator current. Consequently, Equation 9 and Equation 11 can be used to control the speed of the motor by adjusting V_{TPP} and I_{stator}. In this work, the two parameters adjustment is achieved by applying the voltage divider rule, injecting virtual impedance into the power line.

2.2 The Model for the Control Strategy

The series compensator (SC) is designed to be engaged during turbulence (mostly at startup) in DVR mode. This implies that the bypass switch disengages the proposed scheme when the system is operating at normal condition. If the proposed scheme is engaged due to voltage distortion in the system, the SC model injects sufficient magnitude of voltage in phase and in series with the line, while the storage capacitor compensates for voltage sags. The voltage injected by the scheme can be derived as:

$$V_{inj(r,y,b)} = V_{s(r,y,b)} - V_{TPP(r,y,b)} = \alpha V_{dc} - V_{Lf} \quad (12)$$

Where, V_{dc} denotes the DC link voltage, α denotes the modulation index of the proposed model, and V_{Lf} denotes filter voltage.

When the motor starts up, slip is approximately one ($s_p \cong 1$). From Equation 6 and Equation 11, the starting current can be derived as:

$$i_{start} = \frac{V_{TPP}}{(R_{stator} + X_{stator}i) + \left(\frac{((X_m i)(R_{rotor} + X_{rotor}i))}{(X_m i) + (R_{rotor} + X_{rotor}i)}\right)} \quad (13)$$

From Equation 3.13, the electromagnetic starting torque can be computed as:

$$T_{em\_start} = \frac{3pR_{rotor}}{4\pi f} \cdot \left| \frac{X_m i}{R_{rotor} + (X_{rotor} + X_m)i} \right| \cdot I_{start}^2 \quad (14)$$

The starting current is proportional to the terminal voltage per phase while the electromagnetic torque is proportional to the square of the starting current according to Equation 13 and Equation 14, respectively. Consequently, torque is proportional to the square of terminal voltage per phase.

In order to limit the rotational speed and large inrush current during startup, virtual impedance is introduced as illustrated in Figure **4**. The introduction of virtual impedance to the system makes the output impedance a competent variable to regulate terminal voltage per phase and the starting current. Considering the virtual impedance, the starting current can be rewritten as:

$$i'_{start} = \frac{V_{TPP}}{Z_v + Z_{equiv}} = \frac{V_{TPP}}{Z_v + (R_{stator} + X_{stator}i) + \left(\frac{((X_m i)(R_{rotor} + X_{rotor}i))}{(X_m i) + (R_{rotor} + X_{rotor}i)}\right)} \quad (15)$$

Equation 15 has it evidently that starting current can be seamlessly controlled by varying the virtual impedance.

The configuration of the proposed series compensator scheme gives the flexibility for the system to operate in either of the two different modes (virtual impedance mode or voltage compensation mode) based on the state of the three phase electric motor. At normal condition, the virtual resistor in Figure 4 is deactivated, thus causing the line current to be within nominal range. In this case, the proposed serial compensator scheme operates in DVR mode (similar running condition with the conventional methods). Conversely, if there is voltage distortion (mostly at startup), the virtual impedance control is activated. The control system design is presented in Figure 5.

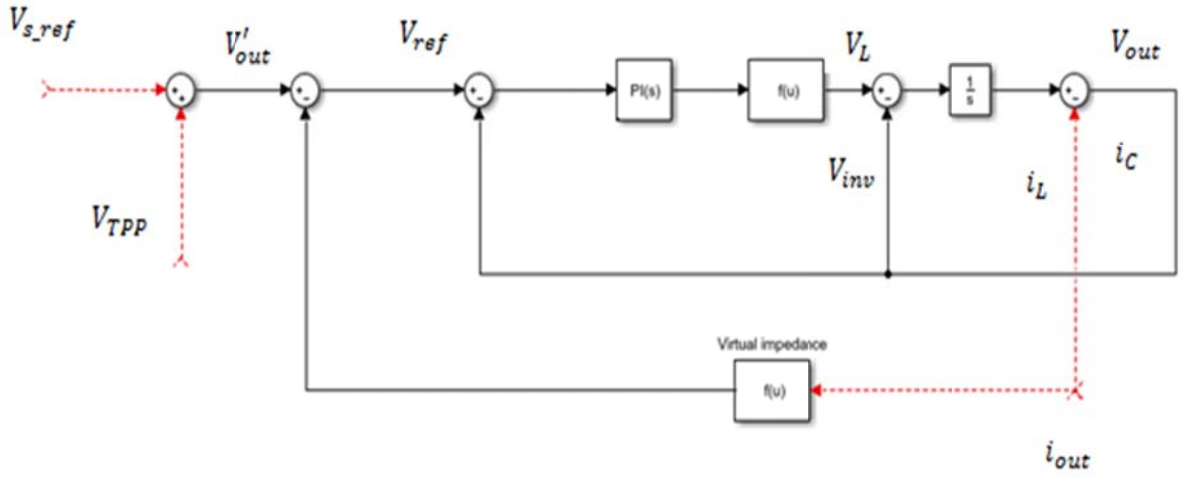

Figure 5: The series compensator control block diagram on the stationary reference frame

In Figure 5, the current through the distribution line and the current through the filter inductor are i_{out} and i_{LF}, respectively; the reference voltages for the power system and the voltage loop are V_{s_ref} and V'_{out}, respectively. The current through the filter capacitor is denoted by i_c, the output voltage of the system is denoted by V_{out}, while V_{inv} denotes the output voltage of the series inverter.

Suppose the switching frequency of the electronic switch is sufficiently high, then the instantaneous value of the AC variable can be used in place of the mean value. By applying Kirchhoff's voltage and current laws, the output voltage, V_{out} of the inverter can be derived as.

$$C_f \frac{dV_{out}}{dt} = i_{Cf} - i_{Lf} - i_{out} \quad (16)$$

$$L_f \frac{di_{Lf}}{dt} = V_{inv} - V_{out} \quad (17)$$

$$V_{inv} = L_f C_f \frac{d^2 V_{out}}{dt} + L_f \frac{di_{out}}{dt} + V_{out} \quad (18)$$

According to Figure 5, the output of the inverter arm can be tracked; consequently, the series inverter output voltage can be expressed as:

$$V_{inv} = V_{ref} + k_p(V_{ref} - V_{out}) + k_I \int (V_{ref} - V_{out})dt \quad (19)$$

The voltage across filter capacitor can be computed as:

$$V_{out} = \frac{(1+k_p)s+k_I}{L_f C_f s^3+(1+k_p)s+k_I} V_{ref} - \frac{L_f s^2}{L_f C_f s^3+(1+k_p)s+k_I} i_{out} \quad (20)$$

Equation 3.20 can be expressed in terms of voltage gain and output impedance of the inverter as:

$$V_{out} = G_v(s) \cdot V_{ref} - Z_{inv}(s) \cdot i_{out} \quad (21)$$

$$V_{out} = G_v(s) \cdot V_{ref} - (R_{inv} + X_{inv} i) \cdot i_{out} \quad (22)$$

Note that k_I denotes the coefficient of the integral term, k_p denotes the coefficient of the proportional term, $G_v(s)$ denotes the voltage gain, $Z_{inv}(s)$ denotes the output impedance of the series inverter, R_{inv} denotes the equivalent output resistance, X_{inv} denotes the equivalent output reactance.

The virtual impedance controller also checks the current behavior. If the amplitude of the current is greater than the threshold, the controller will be activated. The series compensator is controlled as pure inductance L_v during startup; this is to prevent the series compensator from absorbing real power which can be dangerous to the control system. So $Z_v(s) = L_v \omega i$. If the excitation impedance is neglected, the system impedance angle can be expressed as:

$$\theta = \cos^{-1}\left(\frac{\left(R_{stator}+\frac{R_{rotor}}{s_p}\right)+R_{inv}}{\sqrt{\left(\left(R_{stator}+\frac{R_{rotor}}{s_p}\right)+R_{inv}\right)^2+(X_{stator}i+X_{rotor}i+X_{inv}i+X_vi)^2}}\right) \rho \sqrt{\left(R_{stator}+\frac{R_{rotor}}{s_p}\right)^2+(X_{stator}i+X_{rotor}i+X_vi)^2} = \sqrt{\left(R_{stator}+\frac{R_{rotor}}{s_p}\right)^2+(X_{stator}i+X_{rotor}i)^2} \quad (23)\ (26)$$

$V_s = V_{TPP} + V_{out}$ is the source voltage while V_{out} is the compensation voltage which is orthogonally injected to the load current i_{start}. The system impedance expressed in Equation 23 is achieved by adjusting the virtual impedance, thus, the voltage injected can be expressed as:

$$V_{out} = Z_v \cdot i_{start} \quad (24)$$

After starting the three phase electric motor, the speed of the rotor gradually increases which results in decrease in slip ratio. According to Equation 15, the virtual impedance Z_v can be dynamically modified during startup to limit the starting current.

Consider a series connection between the virtual impedance and the distribution line, and then the terminal voltage can be represented as:

$$V_{TPP} = \left(1 - \frac{Z_v \cdot i_{out}}{V_s}\right) \cdot V_s = \rho \cdot V_s \quad (25)$$

Where ρ represents the ration between V_{TPP} and V_s. The direct starting current is greater than the soft starter current by ρ. Also the direct starting torque is greater than the soft starter torque by square of ρ. i'_{start} and T'_{em} are checked for different values of ρ. For instance, $\rho = 1/16$, and the effect of Z_{inv} is neglected.

and the initial value of the virtual impedance can be expressed as:

$$Z_{v_0} = \sqrt{(1-\rho^2)\cdot\left(R_{stator}+\frac{R_{rotor}}{s_p}\right)+(X_{stator}i+X_{rotor}i)^2} - (X_{stator}i+X_{rotor}i) \quad (27)$$

By considering the initial value of the virtual impedance, the dynamic adjustment process can be derived as:

$$Z_v = Z_{v_0} - \sum_{i=1}^{T} k \cdot J_{v_{0\_i}} \quad (28)$$

Where, J_{v_0} denotes virtual impedance correction factor, T denotes the virtual impedance operating period, and k is governed by the constraint in Equation 29

$$k = \begin{cases} 1, & \Delta I > 0 \\ 0, & \Delta I < 0 \end{cases} \quad (29)$$

Where $\Delta(I = I_{n+1} - I_n$. This can limit the starting current to a substantial value.

2.3 Model Simulation and Evaluation

In order to validate the proposed system, the model simulation is conducted using matrix laboratory (MATLAB). First, the SCR switching circuit was modeled in SIMULINK as presented in Figure 6. The virtual impedance controller SIMULINK model is presented in Figure 7.

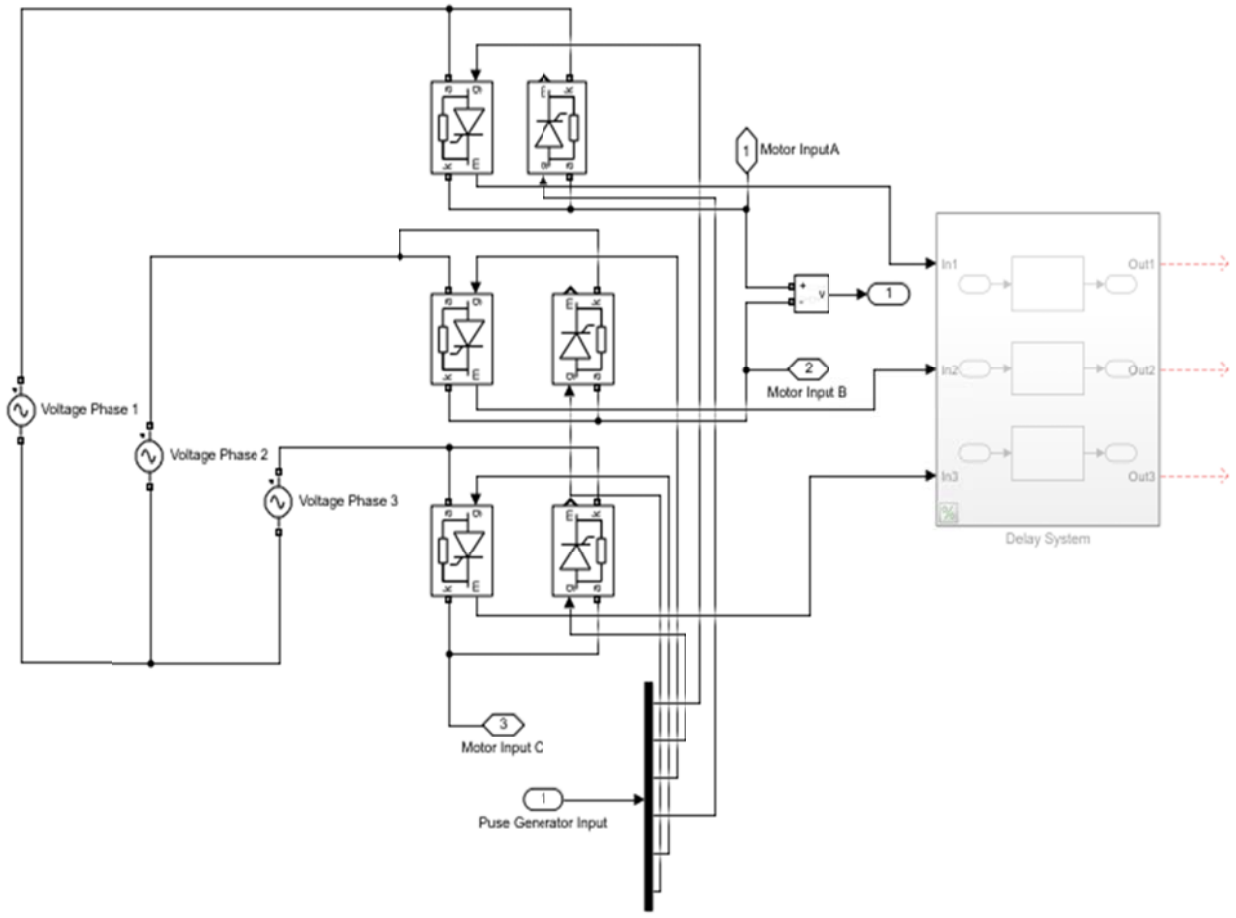

Figure 6: The SIMULINK Model of the SCR Switching Unit

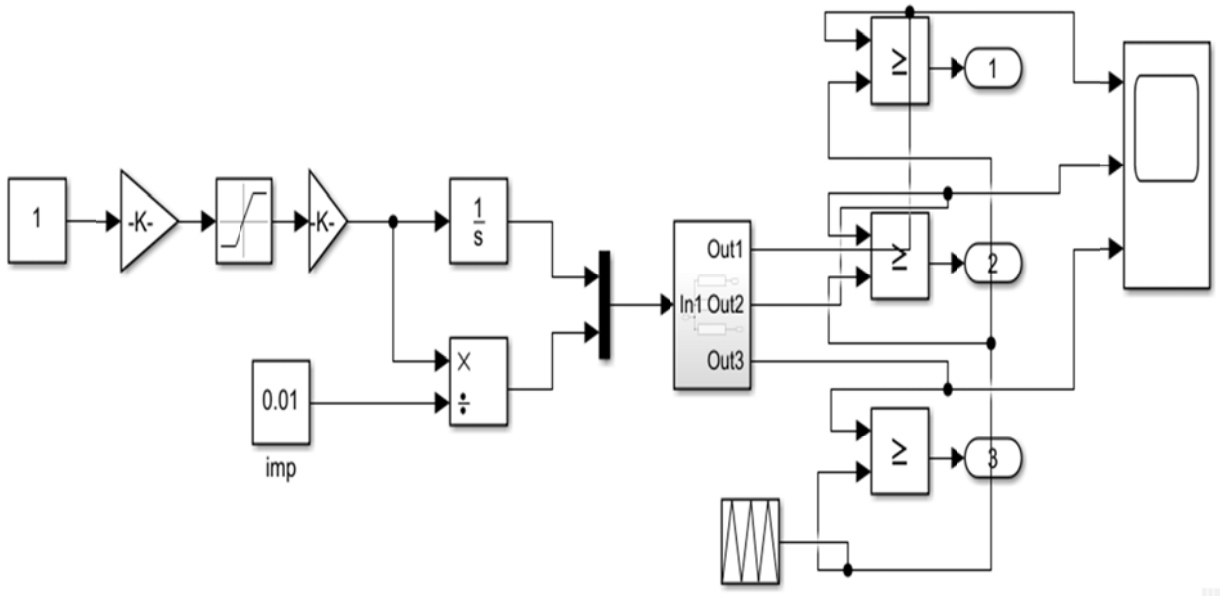

Figure 7: The SIMULINK Model of the Virtual Impedance Control System

In Figure 8, SIMULINK model of the rotor speed controller is presented. This model uses a Proportional Integral Derivative controller (PID) to control the speed of the rotor. The SIMULINK model of the overall system is presented in Figure 9. In the overall system, the three phase electric motor is presented and connected to the specified and modeled controllers to have the desired results.

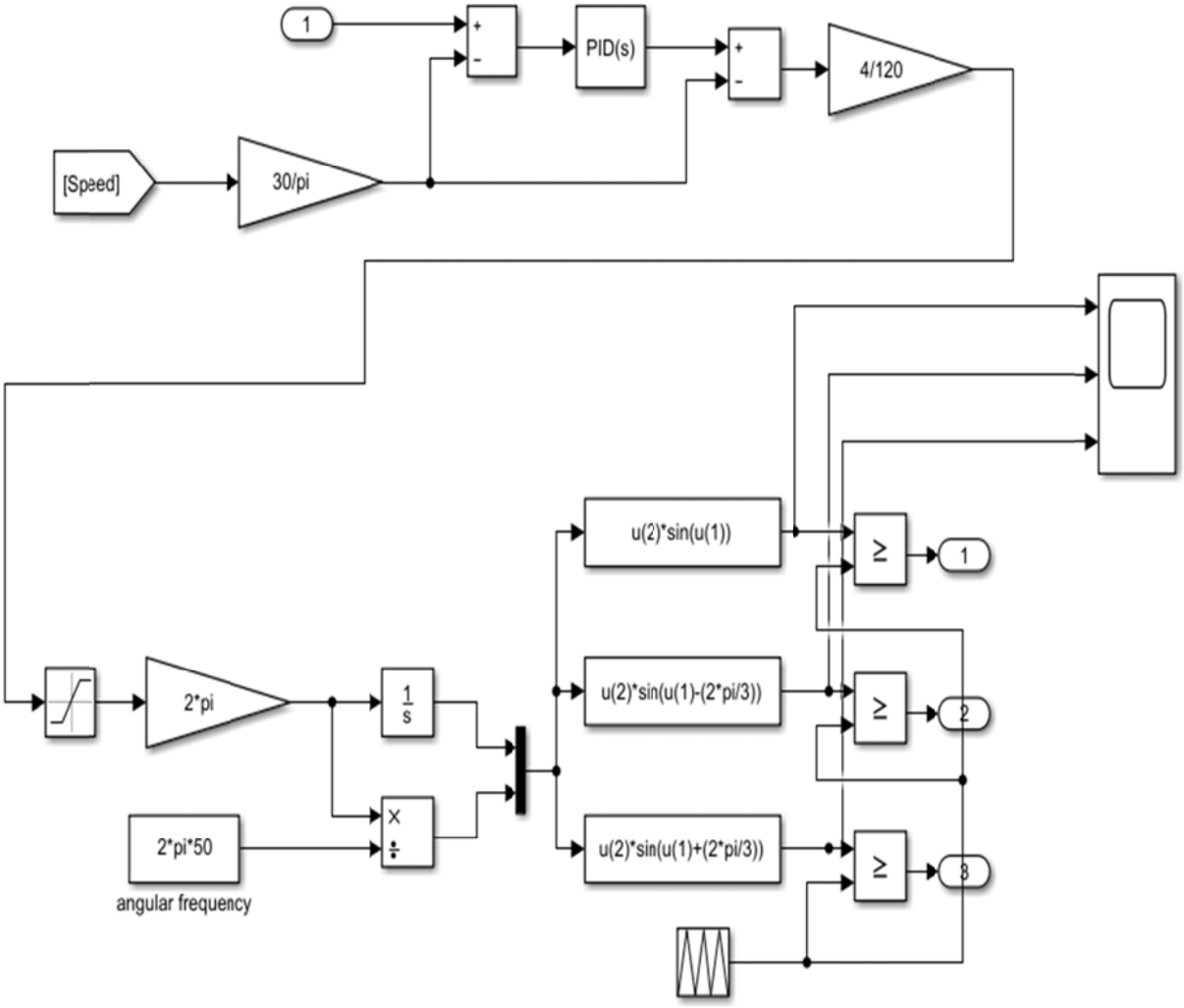

Figure 8: The SIMULINK Model of the Rotor Speed Control System

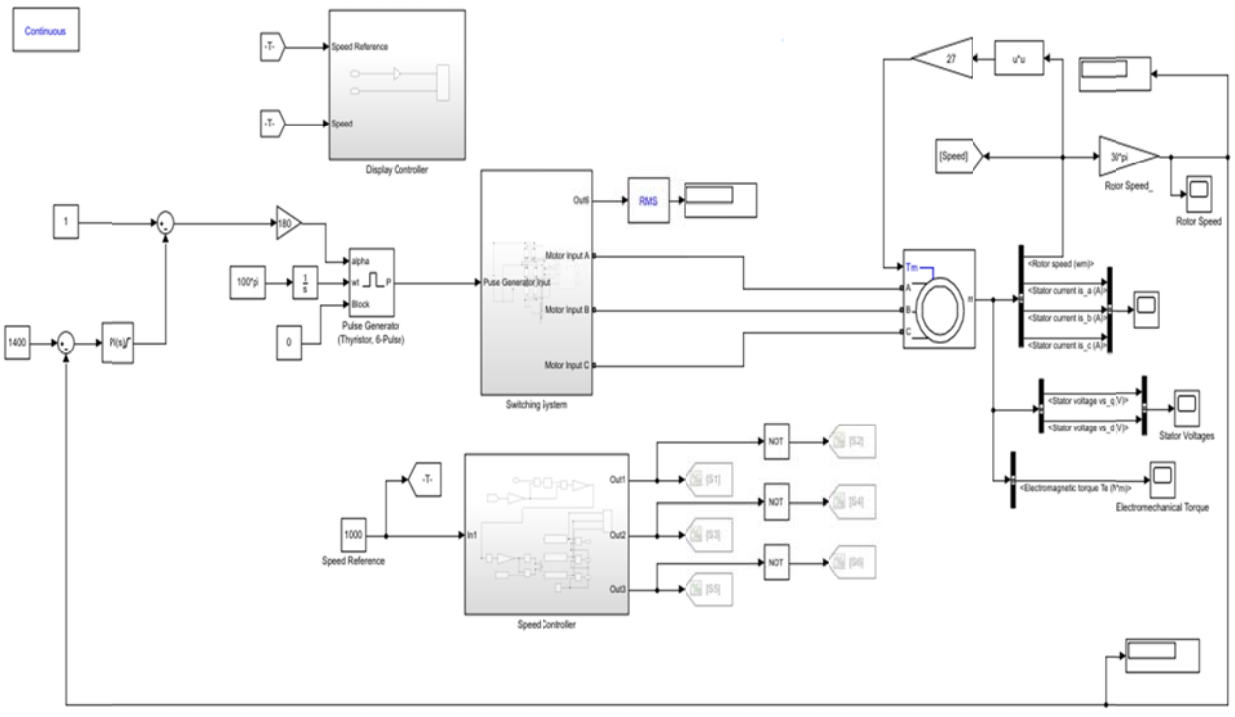

Figure 9: The SIMULINK Model of the Overall System

3. RESULTS AND DISCUSSION

3.1 SIMULATION PARAMETERS

The system is modeled and simulated in MATLAB and the simulation parameters used are as presented in Table 1

Table 1: Parameters Used in the Simulation

Parameter	Value
Stator resistance	0.51Ω
Stator inductance	$0.003H$
Rotor resistance	1.09Ω
Rotor inductance	$0.004H$
Mutual inductance	$0.052H$
Motor rated power	$10KW$
Switching frequency	$5kHz$
L-filter	$3mH$
C-filter	$300\mu F$
Line impedance	0.01Ω
Source voltage	$480v$
Link capacitor	$5000\mu F$
Friction factor	$0.09N.m.s$

In order to observe the switching or transition characteristics of the system between the motor current and the DOL starter, the output waveforms in Figure 10 (result for the proposed method) and Figure 11 (result for the conventional method) are presented. It is seen that when the three phase electric motor is operated using the conventional method, there is a large inrush starting current up to $3700A$ at the initial stage which goes gradually to steady state in about $10\ seconds$. The current waveform in Figure 11 settles at about $500A$. However, when the proposed solution is applied, the current waveform does not just have a quick settling time (at about 0.3 seconds), but the settling amplitude is about $150A$ which is about 70% optimization.

Also, Figure 12 shows the corresponding torque when the proposed technique is applied. Usually, the torque is very high since the three phase electric motor requires large amount of energy at start up. From Figure 12, the torque oscillates from an initial value of $175Nm$ and it is gradually driven by the control scheme to attain a steady state of zero when the three phase motor is fully started.

3.2 Switching Characteristics Between Motor Current and DOL Starter

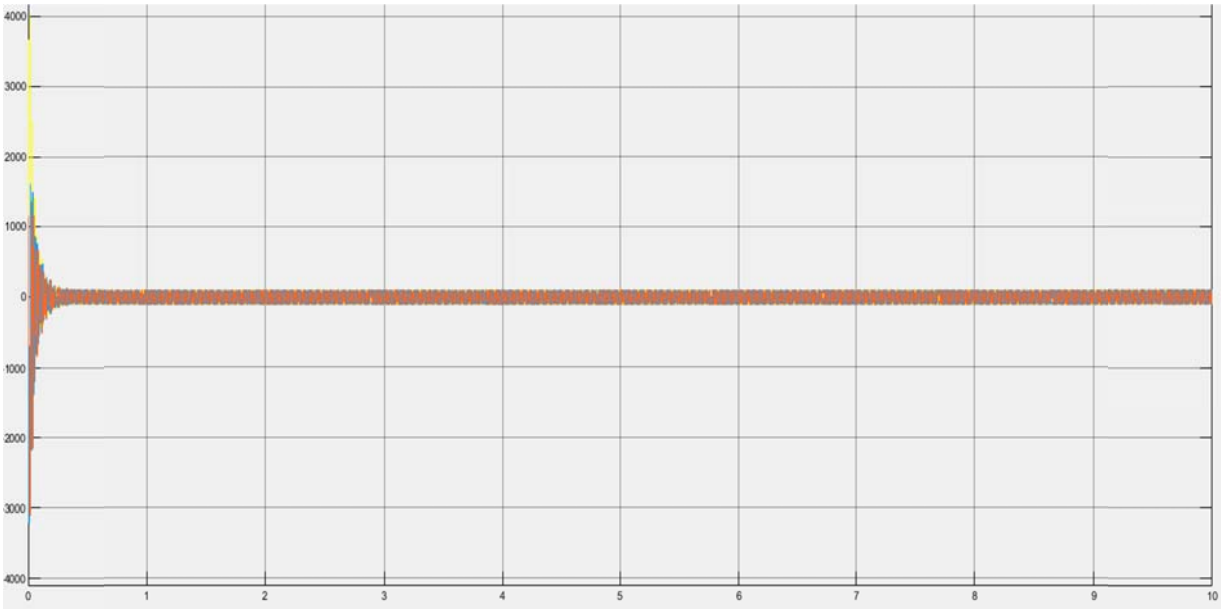

Figure 10a: Switching Characteristics of the Motor Starting Current Based on the Proposed Method.

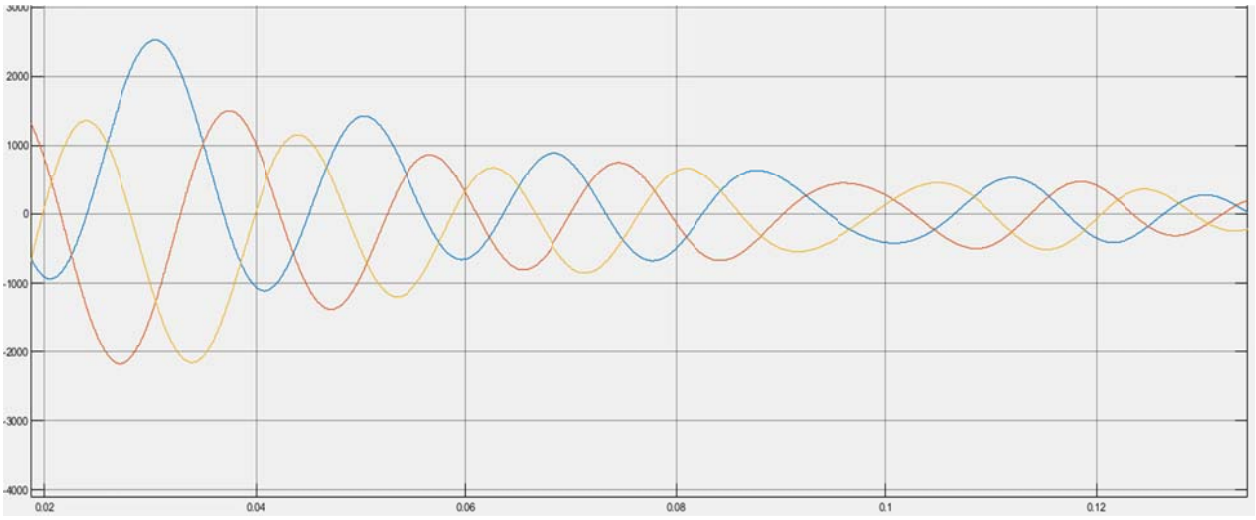

Figure 10b: Switching Characteristics of the Motor Starting Current Based on the Proposed Method.

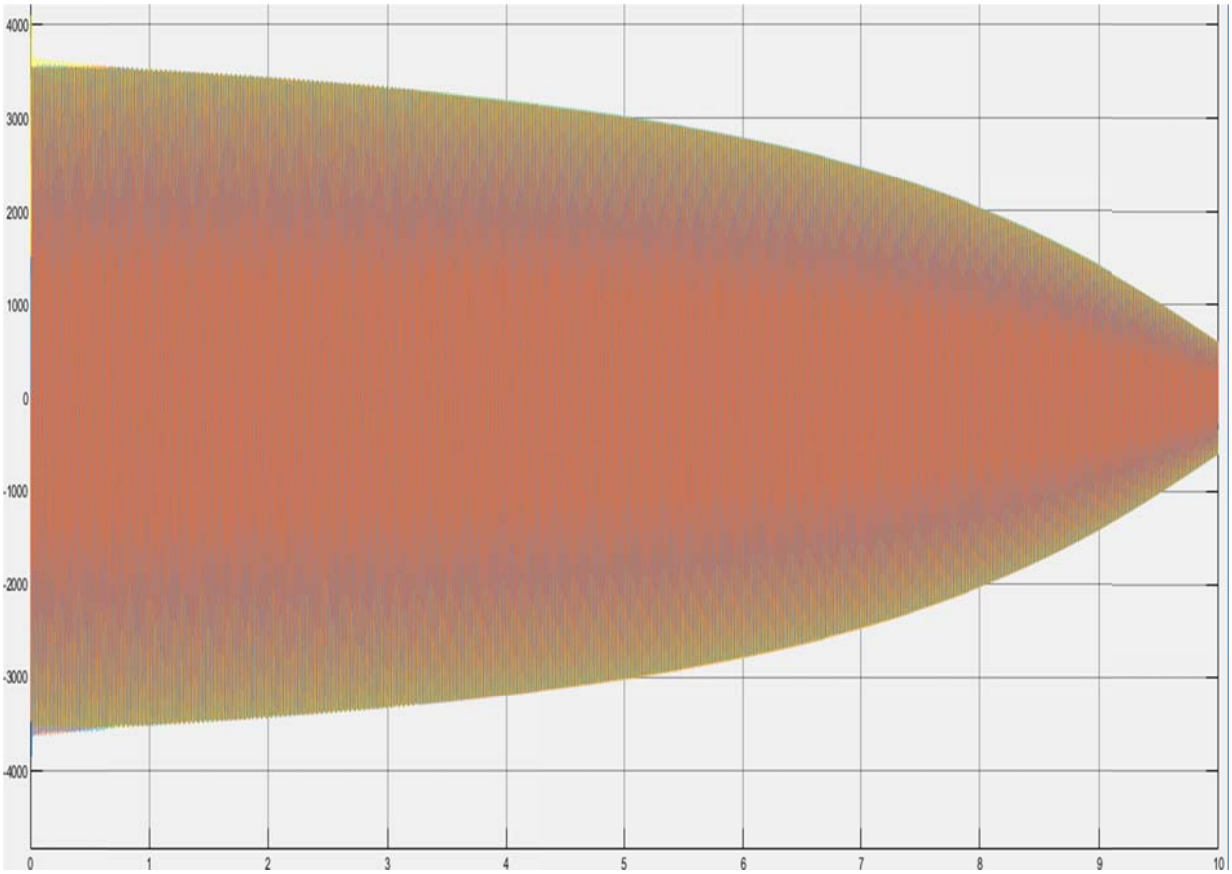

Figure 11: Switching Characteristics of the Motor Starting Current Based on Conventional Method.

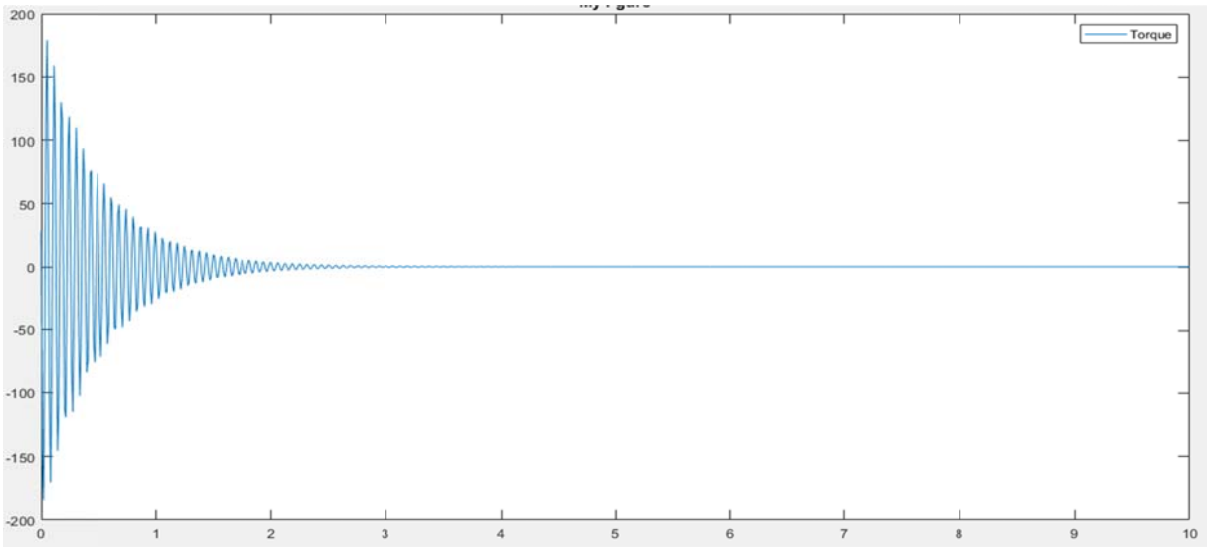

Figure 12: Corresponding Torque for the Switching Characteristics

3.3 Voltage Characteristics of the System

The zoomed graph of the line voltages of the system when the proposed scheme is applied are shown in Figure 13 while Figure 14 shows the stator voltage on the D-frame and Figure 15 shows the stator voltage on the Q-frame . As expected, the line voltages oscillates around $\pm 470v$. The system voltages as shown in Figures 13 to Figure 15 indicate that the proposed system does not have significant influence on voltages when the system is running at nominal speed.

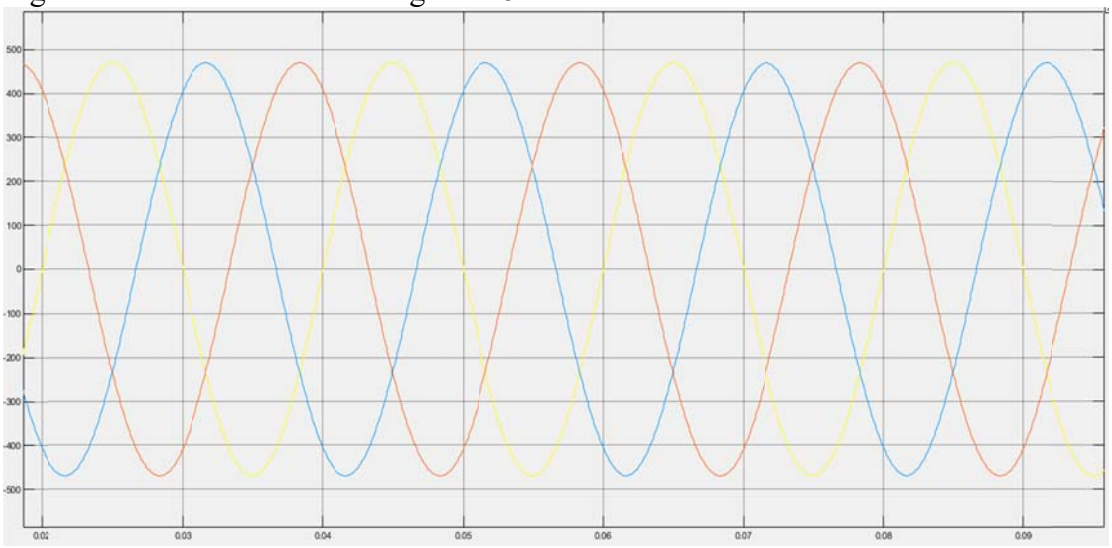

Figure 13: Line Voltages of the System (Zoomed)

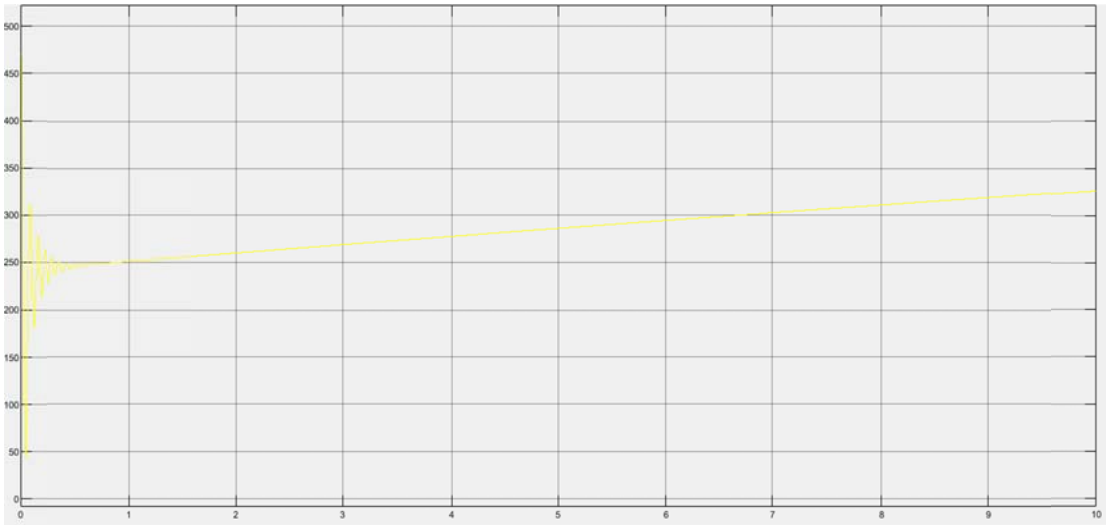

Figure 14 : Stator Voltage (D-Frame)

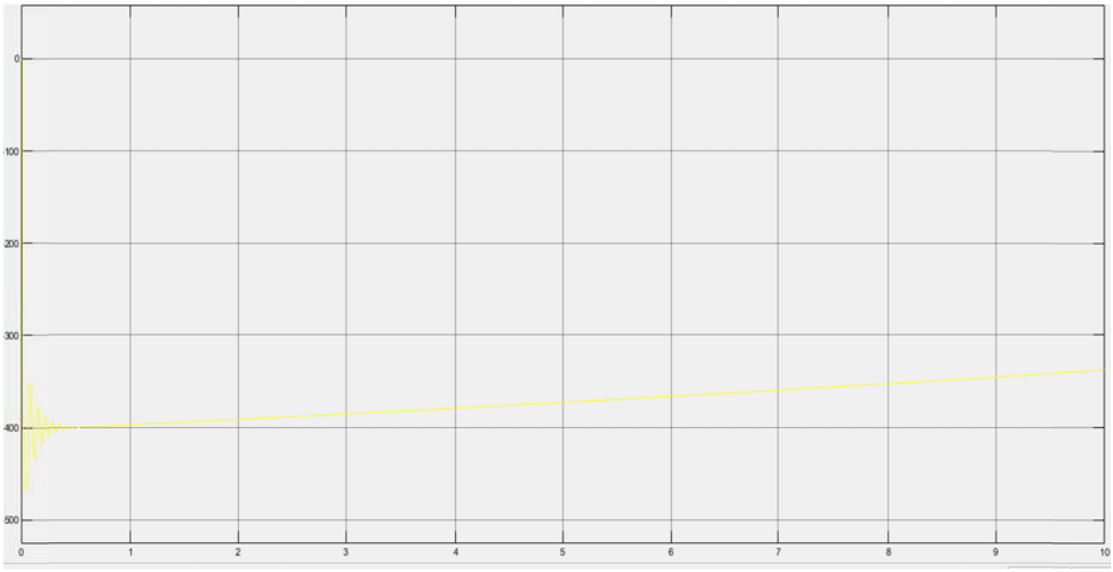

Figure 15: Stator Voltage (Q-Frame)

3.4 Current Characteristics of the System

The currents behaviors of the system were also investigated and the line currents are presented in Figure 16. As shown in Figure 16, the line current oscillates initially around $\pm 800A$, then settles at steady state around $\pm 180A$ in $0.2\,seconds$. However, line current without the proposed system presented in Figure 17 exhibits different characteristics. The current tends to begin from zero and then rise to attend a steady state of about $\pm 220A$ in 0.08 seconds. The current starts from zero in the conventional case following the running speed of the rotor. On the other hand, the proposed method does not engage motor system until the current rises to a sufficient magnitude. This makes it safe for loads connected to the system.

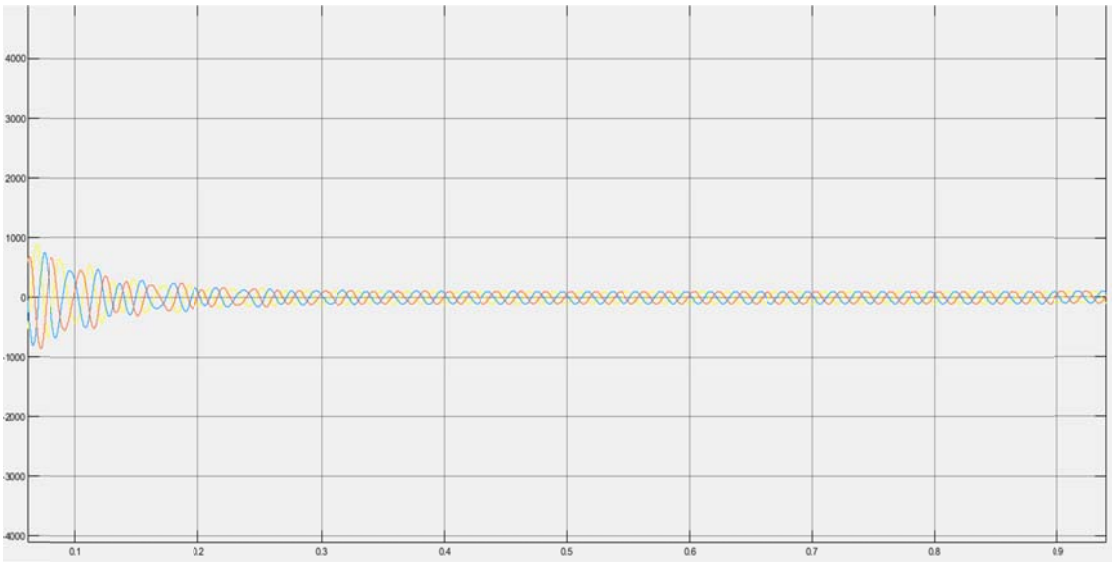

Figure 16: System Line Currents (Proposed Technique).

3.5 The system line currents, electromagnetic torque and rotor speed at normal operation

The graphs in Figure 17 to Figure 22 show the results for the system line currents , electromagnetic torque and rotor speed at normal operation (or steady state). In the results shown in Figure 17 to Figure 22, the proposed system behaviours does not differ from the existing or convention system. Notably, the solution presented in this work is only relevant when the three phase electric motor is about to start. This is the time it draws enormous current, and the aim of this study is to minimize the huge current (using the soft start technique). As such, once the three phase electric motor is started and runs on normal operating speed, everything becomes normal as is obtainable in the phase electric motor with the conventional Direct On-Line (DOL) Starter method.

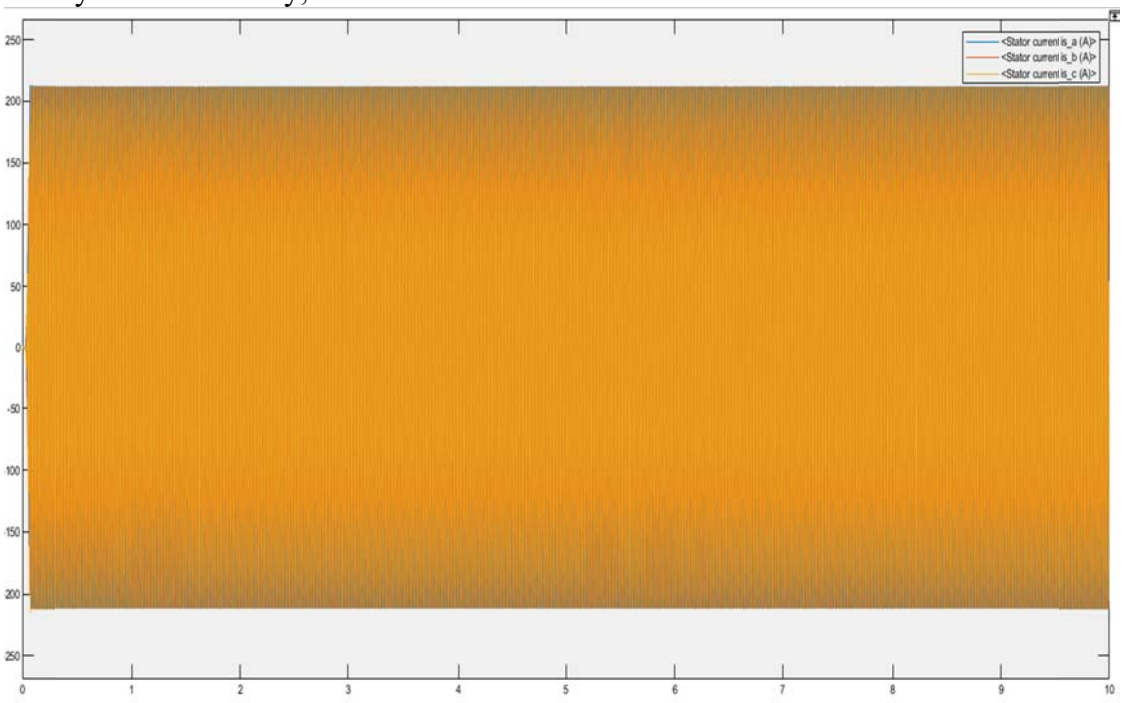

Figure 17: System Line Currents (Conventional Technique).

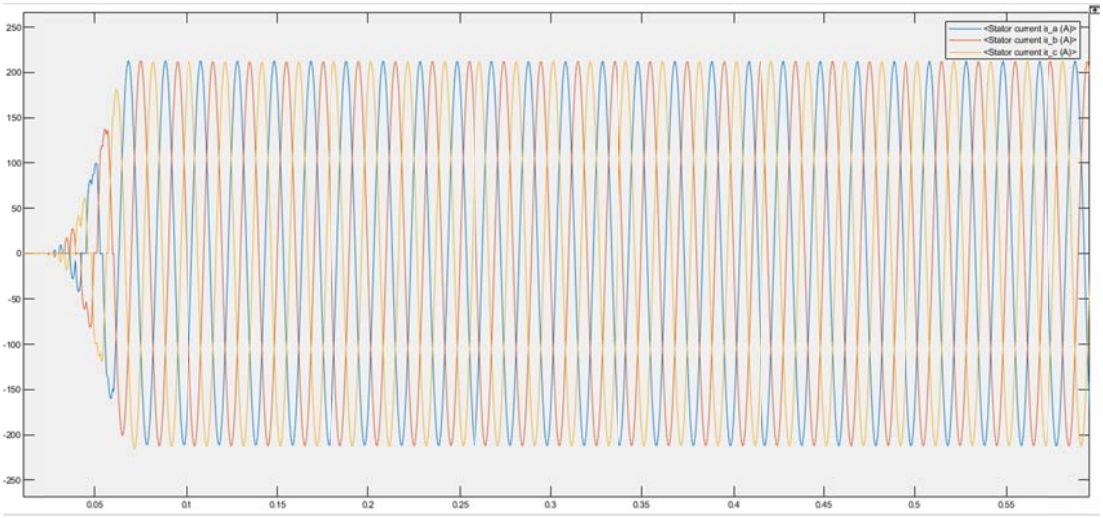

Figure 18: System Line Currents (Conventional Technique – Zoomed).

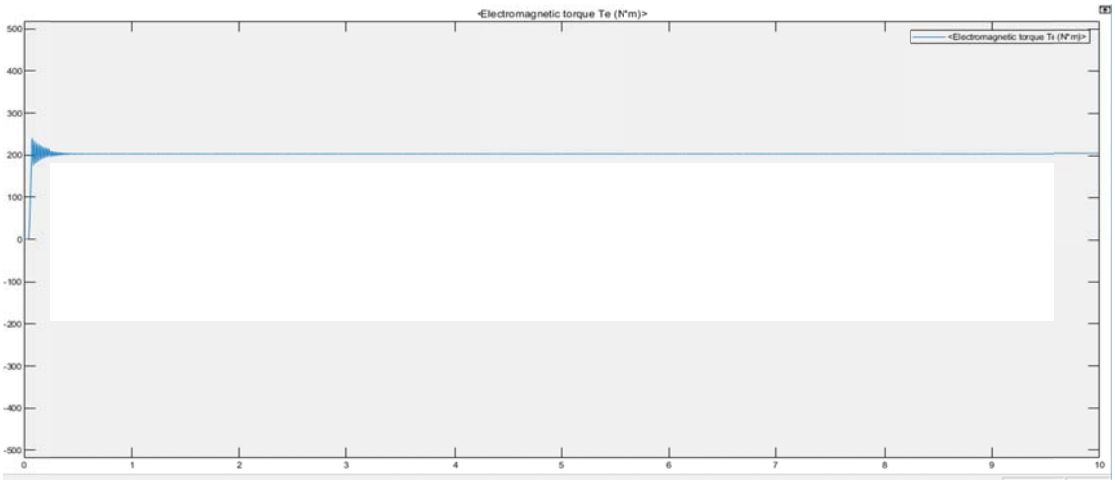

Figure 19: Line Currents Electromagnetic Torque

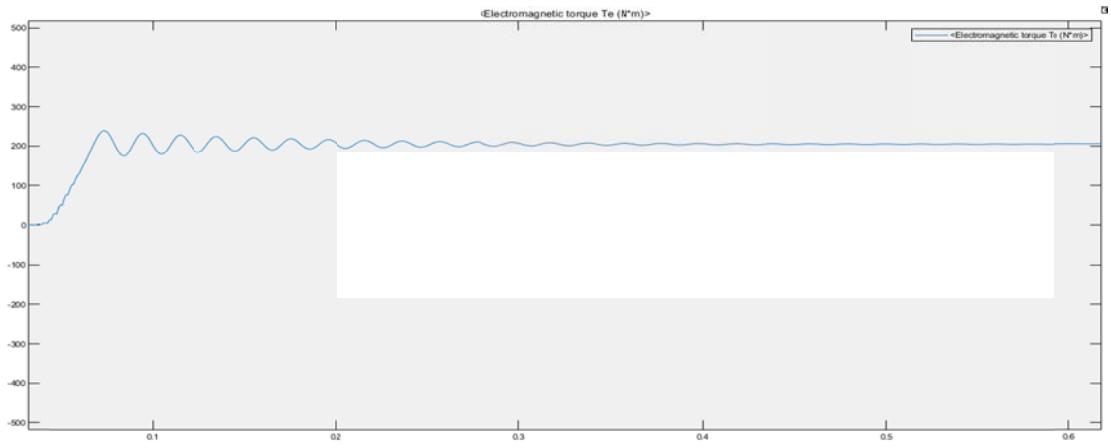

Figure 20: Electromagnetic Torque (Zoomed)

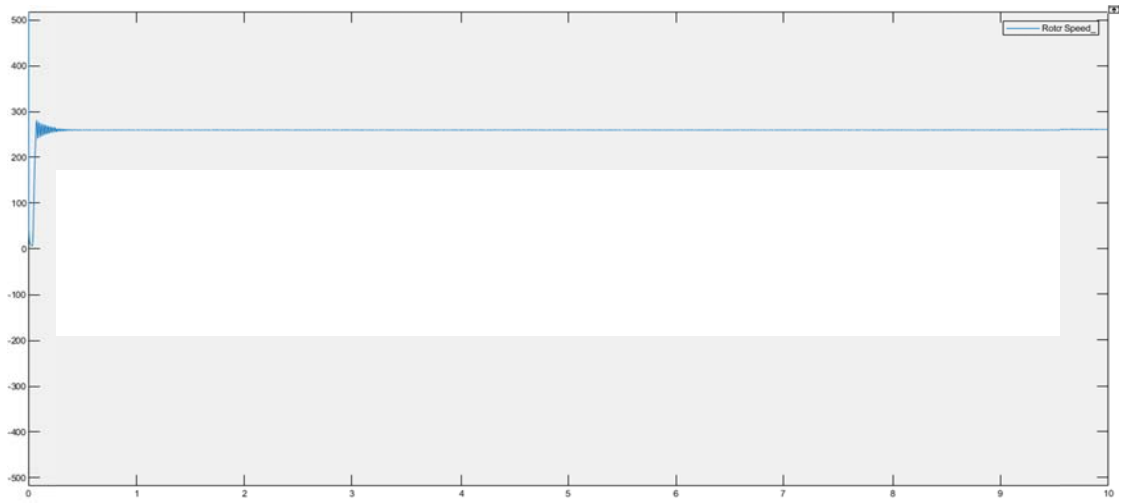

Figure 21: Line Currents , Electromagnetic Torque Rotor Speed

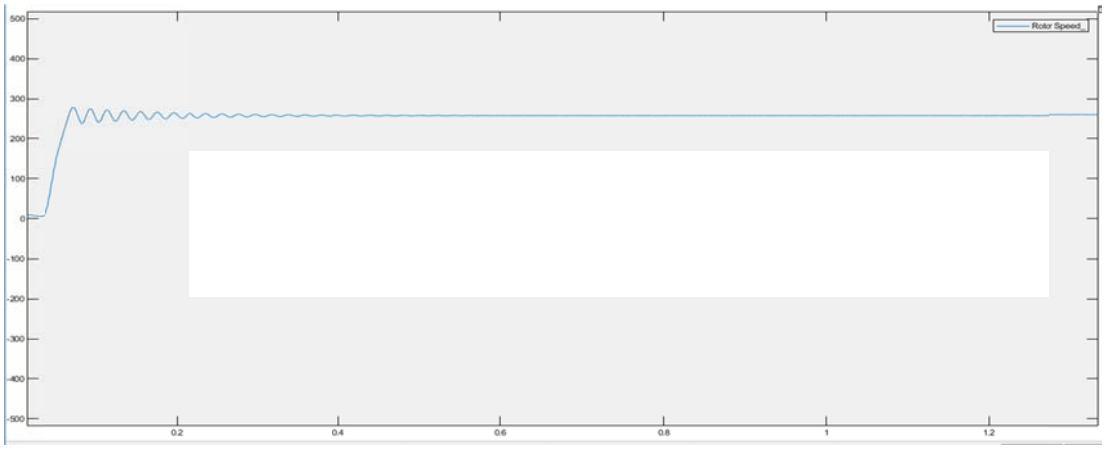

Figure 22: Rotor Speed (Zoomed)

4. CONCLUSION

This study presents the design of electric circuitry for Thyristor-based Direct On-Line (DOL) Starter for three phase electric motor which is meant to address the problems associated with the existing conventional Direct On-Line (DOL) Starter. Notably, the conventional Direct On-Line (DOL) Starter is usually designed and constructed with electromechanical components such as Isolator Gear Switch Fuses (IGSF), Molded Case Circuit Breaker (MCCB), Electromagnetic Contactor, Thermal Overload Relay (TOR), Miniature Circuit Breaker (MCB). The two major challenges identified in which the proposed solution tackles are: voltage sag and large inrush currents. Consequently, the proposed solution is optimized to operate in compensation mode when there is voltage sag, and virtual impedance state if high inrush current is detected. The solution proffered in this research is an improvement to the existing systems. In addition to its effectiveness, it is also a cost effective solution.

In addition, the results for the system line currents, electromagnetic torque and rotor speed at normal operation (or steady state) show that the proposed system behaviours does not differ from the existing or convention system at steady state. Notably, the solution presented in this work is only relevant when the three phase electric motor is about to start. This is the time it draws enormous current, and the aim of this study is to minimize the huge current (using the soft start technique). As such, once the three phase electric motor is started and runs on normal operating speed, everything becomes normal as is obtainable in the phase electric motor with the conventional starter method.

REFERENCES

1. Bala Murali Krishna, V., & Vuddanti, S. (2021). Identification of the best topology of delta configured three phase induction generator for distributed generation through experimental investigations. *International Journal of Emerging Electric Power Systems*, *23*(3), 329-341.
2. Wang, P., Hua, W., Zhang, G., Wang, B., & Cheng, M. (2021). Principle of flux-switching permanent magnet machine by magnetic field modulation theory part I: Back-electromotive-force generation. *IEEE Transactions on Industrial Electronics*, *69*(3), 2370-2379.
3. Wang, P., Hua, W., Zhang, G., Wang, B., & Cheng, M. (2021). Principle of flux-switching PM machine by magnetic field modulation theory part II: Electromagnetic torque generation. *IEEE Transactions on Industrial Electronics*, *69*(3), 2437-2446.
4. Nazarychev, A. N., Novoselov, E. M., Polkoshnikov, D. A., Strakhov, A. S., & Skorobogatov, A. A. (2020). A method for monitoring the condition of rotor windings in induction motors during startup based on stator current. *Russian Journal of Nondestructive Testing*, *56*, 661-667.
5. Nazarychev, A. N., Novoselov, E. M., Polkoshnikov, D. A., Strakhov, A. S., Skorobogatov, A. A., & Pugachev, A. A. (2020). Experimental determination of diagnostic signs of damage to the rotor windings of high-voltage power plant motors in startup mode. *Russian Journal of Nondestructive Testing*, *56*, 408-416.
6. Satria, M. A., & Andre, A. D. (2022). ANALISA SISTEM STARTING DOL (DIRECT ON LINE) PADA MOTOR LISTRIK PT. SEMEN BATURAJA. *Jurnal Multidisipliner Bharasumba*, *1*(03 October), 395-402.
7. Gavali, P. S., Kamble, R. A., Chin-chawade, V. M., & Rawal, C. S. (2020). Operate Direct on Line Starter Using GSM. *International Journal of Research in Engineering, Science and Management*, *3*(1).
8. Ashour, H. A., & Ibrahim, R. A. (2007, September). Implementation and analysis of microcontroller based soft starters for three phase induction motors. In *EUROCON 2007-The International Conference on" Computer as a Tool"* (pp. 2193-2199). IEEE.
9. Faizal, M. (2016). An Innovative Extinction Angle Control Technique for Soft Starting the Three Phase Squirrel Cage Induction Motor. *Journal of Electrical Engineering & Technology*, *11*(5), 1179-1189.
10. Stephen, D. D. (1988). Ancillary equipment. In *Electric Motor Handbook* (pp. 393-431). Butterworth-Heinemann.
11. Gajera, K., Adeshara, K., & Soni, S. (2021). Efficient and Economically Optimized Way to Limit Inrush Current in an Induction Motor Using Solid-State Devices. In *Advances in Automation, Signal Processing, Instrumentation, and Control: Select Proceedings of i-CASIC 2020* (pp. 859-871). Springer Singapore.
12. Cadirci, I., Ermis, M., Nalcacl, E., Ertan, B., & Rahman, M. (1999). A solid state direct on line starter for medium voltage induction motors with minimized current and torque pulsations. *IEEE Transactions on Energy Conversion*, *14*(3), 402-412.
13. Mbunwe, M. J., Ogbuefi, U. C., Anyaka, B. O., & Ayogu, C. C. (2018). Protection of a disturbed electric network using solid state protection devices. In *Proceedings of the World Congress on Engineering and Computer Science* (Vol. 1).
14. Ukani, N., Jani, K., Chauhan, V., Bhatti, K., & Dhameliya, K. (2014). MODELING & IMPLEMENTATION OF INDUCTION MOTOR SOFT STARTER.
15. Ginart, A., Esteller, R., Maduro, A., Pinero, R., & Moncada, R. (1998, February). Performance improvement in AC-AC SCR controller. In *APEC'98 Thirteenth Annual Applied Power Electronics Conference and Exposition* (Vol. 1, pp. 308-314). IEEE.